Chemical Engineering Journal 162 (2010) 910–918

Contents lists available at ScienceDirect

Chemical Engineering Journal

journal homepage: www.elsevier.com/locate/cej

Selective recognition of 2,4-dichlorophenol from aqueous solution by uniformly sized molecularly imprinted microspheres with β-cyclodextrin/attapulgite composites as support

Jianming Pan, Xiaohua Zou, Xue Wang, Wei Guan, Yongsheng Yan *, Juan Han

College of Chemistry and Chemical Engineering, Jiangsu University, Xuefu Road 301#, Zhenjiang 212013, China

ARTICLE INFO

Article history:
Received 22 April 2010
Received in revised form 24 June 2010
Accepted 25 June 2010

Keywords:
Surface-imprinting technique
Uniformly sized molecularly imprinted microspheres
2,4-Dichlorophenol
Selective recognition
β-Cyclodextrin/attapulgite composites

ABSTRACT

In this study, uniformly sized molecularly imprinted microspheres (MIP) using β-cyclodextrin/attapulgite composites as support were prepared for recognitive adsorption of 2,4-dichlorophenol (2,4-DCP) from aqueous solution. Characterization of MIP were achieved by FT-IR spectra, SEM micrographs, nitrogen adsorption–desorption analysis, EDX measurement and elemental analysis. Equilibrium data, at various temperatures, were described by the Langmuir, Freundlich and Dubinin–Radushkevich isotherm models. The thermodynamics parameters (positive values of ΔH° and ΔS°, negative values of ΔG°) indicated that binding system for MIP was endothermic, entropy gained and spontaneous. Kinetic properties were successfully investigated by pseudo-first-order model, pseudo-second-order model, intraparticle diffusion equation, initial adsorption rate, half-adsorption time and activation energy. A diffusion-controlled process as the essential adsorption rate-controlling step was also proposed. MIP could be reused four times without significant loss in adsorption capacity. The selectivity of MIP also demonstrated higher affinity for target 2,4-DCP over competitive phenolic compounds than that of non-imprinted polymers (NIP).

1. Introduction

The control of water quality is one of the most critical issues in the fields of environmental science and technology. Phenolic compounds can be released into the environment directly and indirectly, such as industrial effluents, municipal sewage and transitional products from natural and synthetic chemicals, including herbicide, pesticide, antiseptic and pharmacy residues [1]. In recent years, phenolic compounds, especially chlorophenols, have been detected in surface water and groundwater in both Asia and Europe [2]. Thus, chlorophenols have been listed in dangerous substances into the aquatic environment. In regular monitoring, selective recognition and removal of target chlorophenols from complex matrices in environmental water samples prior to the detection of trace amount phenolic pollutants is frequently required. Thus, the great priority has been given to the development of novel molecular recognition and selective separation technique.

Molecular imprinting is a convenient and powerful technique to synthesize molecularly imprinted polymers (MIP) which provides artificial receptor-like binding sites for template molecules. These potential binding sites were generated by polymerizing functional monomer and mixed with template molecules in the presence of a cross-linking agent. Subsequently, the removal of template molecules leaves behind imprinted cavities inside the polymer which is complementary in shape, size and functional groups to the template molecules [3,4]. Traditionally, MIP, prepared by bulk polymerization, exhibits highly selective recognition but with poor site accessibility to the target molecules, as the template molecules and functional groups are totally embedded inside the thick polymer network and the binding kinetics is low [5]. Moreover, the conventional bulk polymerization is complicated and time-consuming. Therefore, much attention has been paid to the novel surface-imprinting technique.

Surface-imprinting technique first proposed by Takagi's group in 1992 [6]. Subsequently, surface-imprinting process based on inorganic matrix materials (i.e. SiO_2, TiO_2, α-Al_2O_3, CdS, ZnS quantum dots, carbon nanotube, silica gel, magnetic Fe_3O_4 and so on) which offered fast mass transfer kinetics was established [7–12]. Attapulgite (ATP) is a hydrated octahedral layered magnesium aluminum silicate mineral, which has a fibrous morphology with siloxane groups in the bulk and silanol groups on its surface [13]. Due to its structural morphology and high surface area, ATP is easy to be modified by surfactants and silane coupling agent. At the same time, ATP is also a potential support material in synthesizing surface-imprinting polymer for its chemical, mechanical and thermal stability together with low cost. β-cyclodextrin (β-CD) is

* Corresponding author. Tel.: +86 511 88790683; fax: +86 511 88791800.
E-mail address: zhenjiangpjm@126.com (Y. Yan).

1385-8947/$ – see front matter.
doi:10.1016/j.cej.2010.06.039

a doughnut-shape cyclic oligosaccharides with a hydrophilic exterior and hydrophobic internal cavity. It has been of considerable interest as a functional monomer in molecular imprinting technique because it can build inclusion compounds with hydrophobic molecules by various types of intermolecular interactions [14].

In this work, β-CD/ATP composites with hydrophilic exterior and hydrophobic internal cavity were allowed to self-assemble with the template 2,4-DCP by bonded β-CD. Then imprinting polymerization was conducted using an assistant monomer (methylacrylic acid, MAA), a cross-linking agent (ethyl glycol dimethacrylate, EGDMA) and initiator (2,2′-azobisisobutyronitrile, AIBN). Bonded β-CD and MAA could form complexes with 2,4-DCP through the hydrophobic interaction and the hydrogen bonding interaction simultaneously. After the removal of template molecules, uniformly sized molecularly imprinted microspheres were obtained. The adsorption properties and capacity were demonstrated by equilibrium and batch adsorption experiments. The selectivity of the obtained microspheres was elucidated by performing adsorption experiments over competitive phenolic compounds. Moreover, the regeneration of MIP was evaluated.

2. Materials and methods

2.1. Instruments and apparatus

Infrared spectra (4000–400 cm^{-1}) was recorded on a Nicolet NEXUS-470 FT-IR apparatus (USA). Energy dispersive X-ray spectroscopy (EDX) (SAIMADZU, SSX-550 instrument) was used to observe the chemical composition of products. Nitrogen adsorption–desorption analysis was done at 77 K on a Micromeritics TriStar 3000 porosimeter (Norcross, GA, USA). The morphology of MIP was obtained by scanning electron microscopy (SEM, S-4800). Vario EL elemental analyzer (Elementar, Hanau, Germany) was employed to investigate the surface elemental composition of the particles. High performance liquid chromatograph (HPLC, Shimadzu, Japan) equipped with a UV detector for the detection of phenolic compounds (phenol, 4-CP, 2,6-DCP and 2,4-DCP). The injection loop volume was 20 μL, and the mobile phase consisted of deionized ultrapure water and methanol with a volume ratio of 45:55. The flow rate of the mobile phase was 1.0 mL min^{-1}. The oven temperature was set at 25 °C and then phenol, 4-CP, 2,6-DCP and 2,4-DCP were detected at 272 nm, 282 nm, 277 nm and 285 nm, respectively.

2.2. Reagents and materials

ATP was supplied by Aotebang International Co. in China. Prior to use, it was activated by calcination at 350 °C for 6.0 h before it was dispersed in 0.1 M NH4Cl for 4.0 h at room temperature. EGDMA (Shanghai Xingtu Chemical Co. Ltd., Shanghai, China) was washed consecutively with 10% aqueous NaOH, water and brine, dried over $MgSO_4$, filtered and then distilled under reduced pressure. AIBN (Shanghai No.4 Reagent & H.V. Chemical Co. Ltd., Shanghai, China) was recrystallized from methanol prior to use. Dimethylformamide (DMF), glycidoxypropyltrimethoxysilane (KH-560), MAA and acetonitrile were all purchased from Chemical Reagent Corporation (Shanghai, China). β-CD and sodium hydrogen (NaH), phenol, 2,4-DCP, 4-chlorophenol (4-CP), and 2,6-dichlorophenol (2,6-DCP) were supplied by Sinopharm Chemical Reagent Co., Ltd. (Shanghai, China). β-CD was recrystallized with distilled water before use. All chemicals were of analytical reagent grade, except for, methanol which was of HPLC grade. Deionized ultrapure water was purified with a Purelab Ultra (Organo, Tokyo, Japan).

2.3. Preparation of β-CD/ATP composites

The schematic illustration of synthetic route for β-CD/ATP composites was displayed in Fig. 1a–c. In the first step, β-CD (3.0 g) was dissolved in 100 mL of anhydrous DMF to which NaH (0.3 g) was added. The mixture was stirred at room temperature until no gas was emitted, and the excessive NaH removed by filtration (Fig. 1a). Thereafter, KH-560 (1.0 g) was added and participated in the coupling reaction accompany with ring-opening process. And then the mixture was magnetically stirred at 90 °C for 5.0 h under nitrogen protection (Fig. 1b). Subsequently, the reaction temperature was increased to 115 °C, and ATP (5.0 g) was added rapidly into the mixture. Then co-condensation between silanols from self-hydrolysis of KH-560 and ATP surface took place simultaneously (Fig. 1c). After being stirred for 12 h, the obtained β-cyclodextrin/attapulgite composites were washed with DMF, methanol and dis-

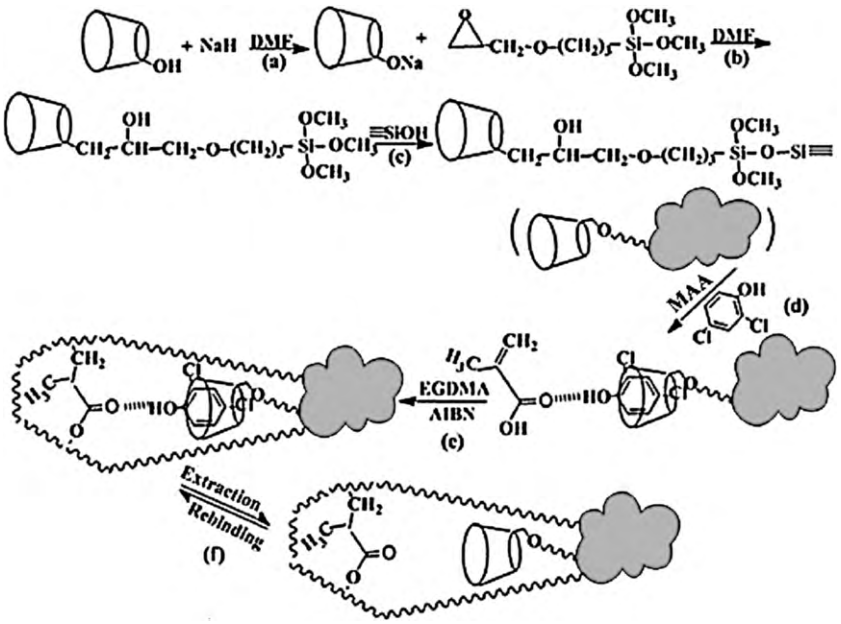

Fig. 1. The synthetic route of the β-cyclodextrin/attapulgite composites and MIP.

tilled water, respectively, and then dried under vacuum at 55 °C.

2.4. Preparation of molecularly imprinted microspheres (MIP)

The schematic illustration of synthetic route for MIP was displayed in Fig. 1d–f. 2,4-DCP (1.0 mmol), β-CD/ATP composites (0.5 g) and acetonitrile (6.0 mL) were transferred into a 25-mL flask. Then the flask was shaken on a constant temperature shaker (25 °C) for 12 h in order to obtain the completely self-assembled β-CD/ATP composites with 2,4-DCP (Fig. 1d). After being filtrated, the saturated composites, 6.0 mL of acetonitrile, assistant monomer MAA (4.0 mmol), EGDMA (20 mmol) and the initiator AIBN (0.66 mmol) were added in turn into a 25-mL thick-walled glass tube. Then, the mixture was purged with oxygen-free nitrogen for 20 min, and then the glass tube was sealed under the nitrogen and placed in an ultrasonic bath for 20 min. Subsequently, the polymerization was allowed to perform for 24 h in a water bath at 60 °C (Fig. 1e). The obtained polymers particles were milled through a 100-mesh screen and washed with the mixture solution of acetonitrile/acetic acid (95:5, v/v) using soxhlet extraction to remove the template molecules (Fig. 1f). Finally, the obtained MIP was dried at 45 °C under vacuum. In comparison, the non-imprinted polymer (NIP) was also prepared as a blank in parallel but without the addition of 2,4-DCP.

2.5. Batch mode adsorption studies

The factors of experimental parameters such as pH, contact time and temperature on the adsorptive removal of 2,4-DCP were studied. For this purpose, 50 mL of aqueous solutions containing 5.0 mg 2,4-DCP were treated in a batch mode of operations, and the concentration of 2,4-DCP in the solvent phase was determined with HPLC. Moreover, the equilibrium adsorption capacity (Q_e, mg g^{-1}) was calculated according to Eq. (1), and the corresponding adsorption isotherms and kinetics curves were drew.

$$Q_e = \frac{(C_0 - C_e)V}{W} \quad (1)$$

where C_0 (mg L^{-1}) and C_e (mg L^{-1}) are the initial and equilibrium concentration of 2,4-DCP, respectively. V (mL) and W (g) are the solution volume and the weight of sorbent, respectively.

2.6. Selective recognition experiments

To measure the selective recognition of 2,4-DCP, the recognition of competitive phenolic compounds were performed. During the experiment, the coexisting phenolic compound (phenol, 4-CP, 2,4-DCP and 2,6-DCP) solution in which each compound contained 5.0 mg was treated according to the procedure of batch mode adsorption studies. The distribution coefficients (K_d), selectivity coefficients (k) and relative selectivity coefficient (k') of phenol, 4-CP and 2,6-DCP with respect to 2,4-DCP can be obtained according to Eqs. (2)–(4).

$$K_d = \frac{Q_e}{C_e} \quad (2)$$

In Eq. (2), K_d (L g^{-1}) represents the distribution coefficient; C_e (mg L^{-1}) represents the equilibrium concentration of the each phenolic compound in solution. The selectivity coefficient (k) for binding of a specific phenolic compound can be obtained according to the following equation:

$$k = \frac{K_{d(2,4\text{-DCP})}}{K_{d(X)}} \quad (3)$$

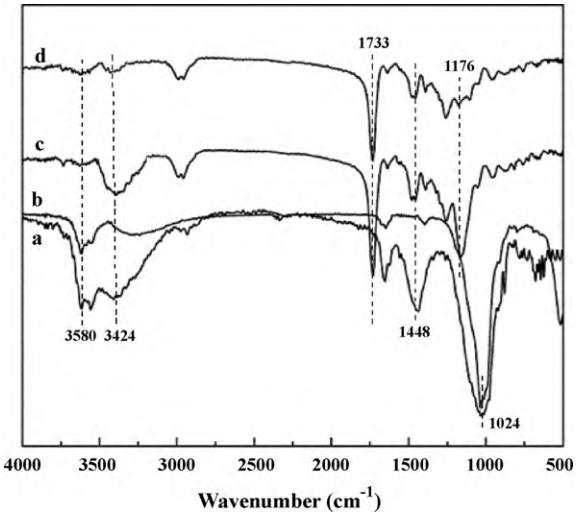

Fig. 2. FT-IR spectra of β-CD/ATP composites (a), ATP (b), MIP before (c) and after (d) leaching 2,4-DCP.

X is the competitive phenolic compound. A relative selectivity coefficient k' can be defined as Eq. (4). k_M and k_N are the selectivity coefficients of MIP and NIP, respectively.

$$k' = \frac{k_M}{k_N} \quad (4)$$

3. Results and discussion

3.1. Characteristics of the MIP

FT-IR spectra of β-CD/ATP composites (a), ATP (b), MIP before (c) and after (d) leaching 2,4-DCP were shown in Fig. 2. For the spectra of β-CD/ATP composites, typical bands of –CH_2– around 1448 cm^{-1} and O–H around 3424 cm^{-1} from β-CD appeared in β-CD/ATP composites, and absorption peak at 3580 cm^{-1} was also attributed to the anti-symmetric stretching modes of molecular water coordinated with the magnesium at the edges of the channel for ATP [15]. Compared with ATP, there were little differences about the locality (1024 cm^{-1}) and intensity of Si–O characteristic feature in β-CD/ATP [16]. The results suggested that β-CD was bonded on the ATP, resulting in the grafted composites β-CD/ATP. For the spectra of MIP before leaching 2,4-DCP, a strong O–H band around 3424 cm^{-1} (typical of phenylic acid) and a C–O band around 1176 cm^{-1} (due to the C–O stretching) were observed, it could be ascribed to self-assembly between 2,4-DCP and bonded β-CD [4]. After leaching 2,4-DCP, weak peaks of O–H and C–O could also be found in MIP, this was possibly caused by the remnants of 2,4-DCP and β-CD/ATP composites. Moreover, the obvious absorption of C=O in cross-linking agent EGDMA located at 1733 cm^{-1}. The results implied that rebinding 2,4-DCP by β-CD/ATP composites and cross-link reaction occurred and polymerization products were successfully introduced onto the β-CD/ATP composites.

SEM was employed to capture the detailed morphology of APT (Fig. 3a), β-CD/ATP composites (Fig. 3b), MIP before (Fig. 3c) and after (Fig. 3d) leaching 2,4-DCP. Compared with ATP, the surface of β-CD/ATP composites was ruleless and agglomerate, which was the result of coating by the products from the cross-linking reaction. From the inset in Fig. 3c and d, it can be found that MIP before and after leaching 2,4-DCP had the similar morphology and size distribution. The particle was aggregated by four uniformly sized microspheres. The actual size of each particle was 8.0 μm, and uniformly sized diameter of microsphere was 4.0 μm.

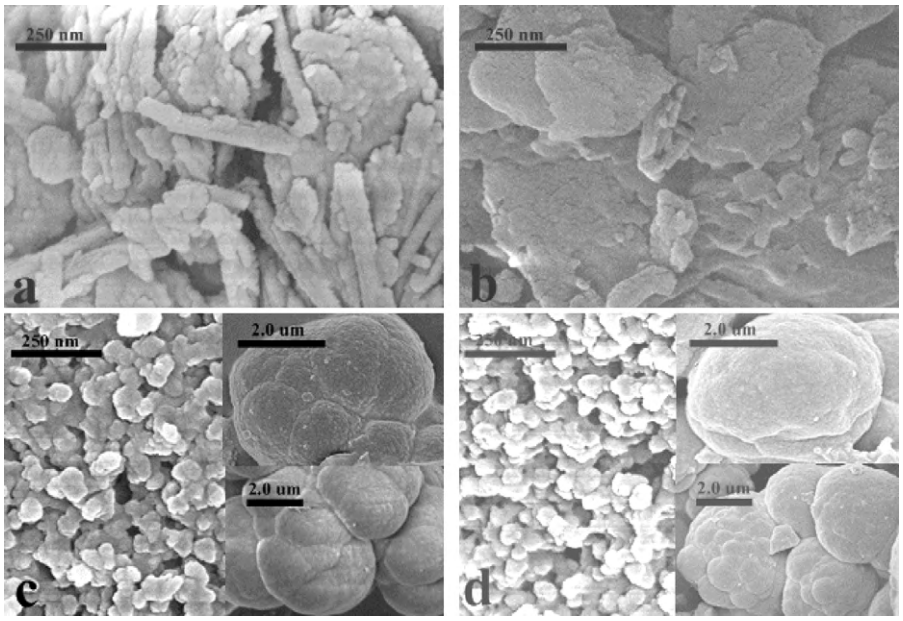

Fig. 3. SEM images of ATP (a), β-CD/ATP composites (b), MIP before (c) and after (d) leaching 2,4-DCP.

Elemental analysis was employed to ascertain each modification. The results were shown in Table SI (Supporting Information). Compared with ATP, the carbon composition in β-CD/ATP composites increased from 1.122 to 5.186%, and hydrogen composition increased from 0.8655 to 1.244%, respectively. The results suggested that β-CD was successfully introduced onto the surface of the ATP. After polymerization, it can be seen that carbon and hydrogen composition were significantly increased. The increase of nitrogen composition may be attributed the AIBN. It can also be found that the elemental composition of the MIP was different from that of the NIP, indicating the 2,4-DCP molecules were not able to completely leached from the MIP. According to the results from EDX analysis (Table SI), 49.09 mg of template 2,4-DCP was immobilized on every gram of the MIP particles, and 15.43% of the template 2,4-DCP was remained on the packing after washing of the MIP.

The specific surface area, total pore volume and average pore diameter for MIP and NIP were also listed in Table SI. They were 116.1 $m^2\,g^{-1}$, 0.3013 $cm^3\,g^{-1}$ and 129.8 å, respectively, for MIP, while these parameters were not obviously different from those of NIP. Therefore, the distinct adsorption properties for MIP and NIP could not entirely be attributed to the morphological differences, but to the imprinting effect. According to the IUPAC definition, MIP and NIP mainly possessed mesopores [17]. Moreover, the average pore diameter for the MIP was slightly higher than that of NIP, also strongly indicating the imprinting effect.

3.2. Effect of pH on the adsorption of 2,4-DCP

Optimization of pH value for adsorption medium plays a vital role in the adsorption studies. The effect of pH value on the treatment of 2,4-DCP by MIP was shown in Fig. SI. The adsorption capacity for MIP decreased with the increase of pH value, while little change was exhibited for NIP. The effect of final pH on ionization of 2,4-DCP in aqueous solution has been reported by Sathishkumar et al. [18]. As a result, adsorption of neutral 2,4-DCP at pH 2.0 by chemisorption was the optimal condition for MIP. When pH value was more than 2.0, owing to the electron-rich influence of 2,4-DCP ions and released OH^-, the interactions between the 2,4-DCP and binding sites of MIP were weakened, which indicating that chemisorption was the preferential mode in adsorption process for MIP [19]. At pH < 2.0, the surface of MIP and 2,4-DCP positively charged, electrostatic repulsion were not benefit for the adsorption system. Little effect of pH value observed for NIP strongly indicated chemisorption was just one of interactions between sorbent and adsorbate.

3.3. Adsorption isotherms

Adsorption isotherm model is significantly important to investigate how adsorbate interact with sorbent. The equilibrium data of MIP and NIP were then fitted to the Langmuir [20], Freundlich [21] and Dubinin–Radushkevich [22] isotherm models. The applicability of the isotherm models to the adsorption behaviours was studied by judging the correlation coefficient (R^2). The adsorption isotherm constants for NIP and MIP at three temperatures were listed in Table 1. Moreover, comparison of Langmuir, Freundlich and Dubinin–Radushkevich isotherm models for 2,4-DCP adsorption onto MIP and NIP using non-linear regression were also illustrated in Fig. 4.

The Langmuir isotherm model assumes uniform adsorption on the surface and is used for describing monolayer adsorption on a surface containing a finite number of identical sites. The linear form is expressed by the following equation:

$$\frac{C_e}{Q_e} = \frac{1}{Q_m K_L} + \frac{C_e}{Q_m} \quad (5)$$

where C_e is the equilibrium concentration of adsorbate in solution ($mg\,L^{-1}$), Q_e is the equilibrium adsorption capacity ($mg\,g^{-1}$), Q_m is the maximum adsorption capacity of the sorbent, K_L represents the affinity constant.

For predicting the favourability of an adsorption system, the Langmuir equation can also be expressed in terms of a dimensionless separation factor R_L defined as follows [20]:

$$R_L = \frac{1}{1 + C_m K_L} \quad (6)$$

where C_m is the maximal initial concentration of adsorbate. The R_L indicates the favourability and the capacity of adsorption system. When $0 < R_L < 1.0$, it represents good adsorption.

Table 1
Adsorption isotherm constants for MIP and NIP.

Adsorption isotherm models	Constants	MIP			NIP		
		298 K	308 K	318 K	298 K	308 K	318 K
Langmuir equation	R^2	0.9992	0.9997	0.9999	0.9921	0.9983	0.9971
	$Q_{m,c}$ (mg g^{-1})	64.94	71.42	79.36	11.55	20.49	21.28
	K_L (L mg^{-1})	0.0667	0.0716	0.1762	0.0126	0.0332	0.0350
	R_L	0.03613	0.03374	0.01399	0.16556	0.07003	0.06667
	ΔQ (%)	3.513	0.6263	1.466	6.781	7.045	4.542
Freundlich equation	R^2	0.8662	0.8710	8210	0.9903	0.9616	0.9690
	K_F (mg g^{-1})	16.7148	16.6150	27.70	1.044	5.105	5.899
	n	4.057	3.765	4.948	2.6253	4.344	4.7348
	ΔQ (%)	4.341	17.44	12.41	5.556	7.948	7.830
Dubinin–Radushkevich equation	R^2	0.9253	0.9084	0.9135	0.8756	0.7660	0.8454
	$Q_{m,c}$ (mg g^{-1})	63.89	72.68	79.89	9.404	17.81	20.36
	K_{DR} (mol^2 kJ^2)	0.0003	0.0002	0.0002	0.0007	0.0006	0.0008
	E (kJ mol^{-1})	40.83	50.00	50.00	26.73	28.87	25.00
	ΔQ (%)	6.670	6.622	6.629	10.55	6.982	6.526

The Freundlich isotherm model is given as follows:

$$\log Q_e = \log K_F + \left(\frac{1}{n}\right) \log C_e \quad (7)$$

where K_F is an indicative constant for adsorption capacity of the sorbent (mg g^{-1}) and the constant $1/n$ indicates the intensity of the adsorption. Value of $n > 2.0$ represents a favourable adsorption condition [23].

In order to further analyze isotherms of MIP with a high degree of rectangularity, Dubinin–Radushkevich isotherm model is considered, and it is described as follows [22]:

$$\ln Q_e = \ln Q_m - K_{DR}\varepsilon^2 \quad (8)$$

where ε can be correlated as

$$\varepsilon = RT \ln\left(1 + \frac{1}{C_e}\right) \quad (9)$$

The constant K_{DR} is related with free energy (E, kJ mol) of adsorption per molecule of the adsorbate when it is transferred to the surface of the solid from infinity in the solution and can be calculated by Eq. (10):

$$E = (2K_{DR})^{-1/2} \quad (10)$$

where R is the gas constant (8.314 J mol^{-1} k^{-1}) and T is the absolute temperature. A plot of $\ln Q_e$ versus ε^2 enables the constants Q_m and E to be obtained. Value of $K_{DR} < 1.0$ represents the rough surface with many cavities, and the great value of E (>40 kJ mol^{-1}) expresses the chemisorption between sorbent and adsorbate.

From Fig. 4, when the equilibrium concentration increased, the equilibrium adsorption capacity (Q_e) of MIP firstly increased sharply, then increased slightly, and finally reached to maximum point. But the adsorption isotherms of NIP were different from MIP in shape. And the Q_e of NIP increased tardily in the whole process. Furthermore, with temperature increased from 298 K to 308 K and 318 K, Q_e of MIP and NIP were elevated obviously, it is probably because high temperature provided more chances for 2,4-DCP molecules to mobilize onto binding sites, and produced the enlargement of pore volume and surface area enabling 2,4-DCP molecules to penetrate further. Moreover, MIP had better applicability for the Langmuir isotherm model while the NIP for Freundlich isotherm model, indicating monolayer molecular adsorption for MIP and multi-molecular layers adsorption for NIP.

3.4. Adsorption kinetics

3.4.1. Adsorption kinetic models

In order to examine the adsorption mechanism such as mass transfer and chemical reaction, the kinetic data obtained were analyzed using pseudo-first-order rate equation and pseudo-second-order rate equation [24,25]. They are described in Eqs. (11) and (12).

$$\ln(Q_e - Q_t) = \ln Q_e - k_1 t \quad (11)$$

$$\frac{t}{Q_t} = \frac{1}{k_2 Q_e^2} + \frac{t}{Q_e} \quad (12)$$

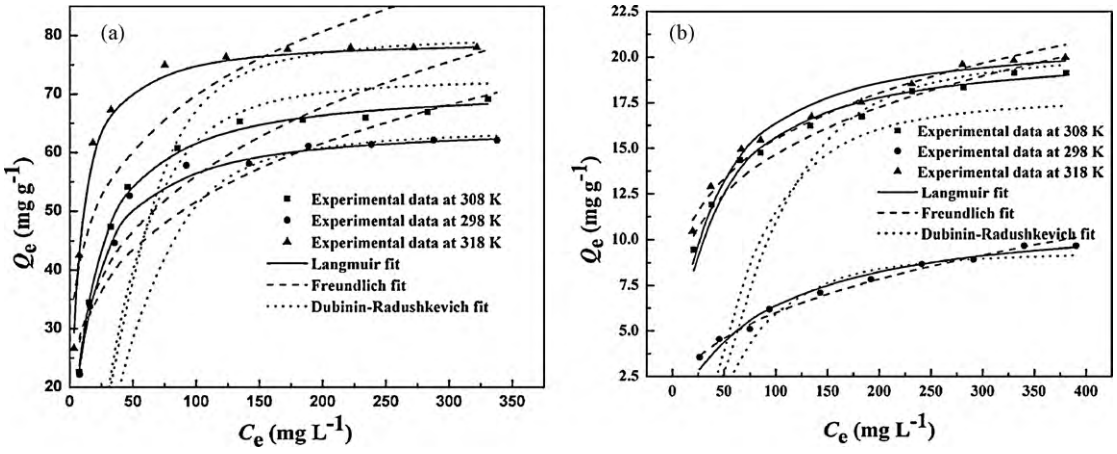

Fig. 4. Comparison of Langmuir, Freundlich and Dubinin–Radushkevich isotherm models for 2,4-DCP adsorption onto MIP (a) and NIP (b) using non-linear regression.

Table 2
Kinetic constants for the Pseudo-first-order equation and Pseudo-second-order equation.

Kinetic models	Constants	MIP			NIP		
		298 K	308 K	318 K	298 K	308 K	318 K
Pseudo-first-order equation	$Q_{e,c}$ (mg g^{-1})	41.34	43.46	44.13	31.01	31.54	29.74
	K_1 (L min^{-1})	0.0043	0.0024	0.0022	0.0035	0.0035	0.0060
	R^2	0.9153	0.9264	0.8894	0.9930	0.9955	0.9949
	ΔQ (%)	2.557	4.345	1.312	4.586	3.281	4.808
Pseudo-second-order equation	$Q_{e,c}$ (mg g^{-1})	45.45	45.25	45.87	29.50	30.30	31.06
	K_2 (g g^{-1} min^{-1})	11.58	11.74	23.53	3.230	3.090	3.980
	R^2	1.000	0.9999	1.000	0.9992	0.9990	0.9997
	ΔQ (%)	0.0245	1.195	1.306	1.431	1.576	0.6039

where Q_e and Q_t are the amount of 2,4-DCP adsorbed (mg g^{-1}) onto sorbent at the equilibrium and time t (min), respectively. Values of k_1 (L min^{-1}) and k_2 (g g^{-1} min^{-1}) are calculated from the plot of $\ln(Q_e - Q_t)$ versus t and t/q_t versus t, respectively.

The adsorption rate constants and linear regression values were summarized in Table 2. The adsorption of 2,4-DCP onto MIP followed pseudo-second-order kinetics because of the favourable fit between experimental and calculated values of Q_e (R^2 values above 0.9999 at different temperature). Low R^2 values of MIP for the first-order kinetic model suggested that 2,4-DCP molecules were strongly held onto the binding sites of MIP by chemical bonds, involving valence forces through sharing or exchange of electrons between sorbent and adsorbate. And it is assumed that the adsorption process was a chemical process, which could be the rate-limiting step in the adsorption process. Furthermore, the data of NIP exhibited good linear relationship with two models mentioned above, indicating the multi-interactions such as physical and chemical adsorption between sorbent and adsorbate.

Fig. 5 shows the plot of the experimental data of the amount of 2,4-DCP adsorbed per unit mass of sorbent against time along the values for the pseudo-first-order and pseudo-second-order kinetic model. Non-linear form of pseudo-second-order kinetic model studied at different temperature also showed the better fit than pseudo-first-order kinetic model for MIP. From Fig. 5, both model lines deviated substantially from the experimental points around the first 30 min for MIP. The observed deviation from experimental data could be attributed to the sharp fall in concentration gradient after the initial rapid adsorption of 2,4-DCP molecules onto the large amount of vacant binding sites [26,27]. Within this time period, it was believed that there was a switch between mass transfer diffusion control and pore diffusion control, and a change in adsorption mechanism may have occurred after the first 30 min for MIP [28,29].

Basted on the second-order model, the initial adsorption rate and time required for the adsorption to half equilibrium value were summarized in Table 3 according to the following equations [30]:

$$u = k_2 Q_e^2 \tag{13}$$

$$t_{1/2} = \frac{1}{k_2 Q_e} \tag{14}$$

Moreover, the second-order rate constant was also used to estimate the activation energy (E_a, kJ mol^{-1}) of the 2,4-DCP adsorption onto MIP and NIP employing Arrhenius equation [30]:

$$\ln k_2 = \ln A - \frac{E_a}{RT} \tag{15}$$

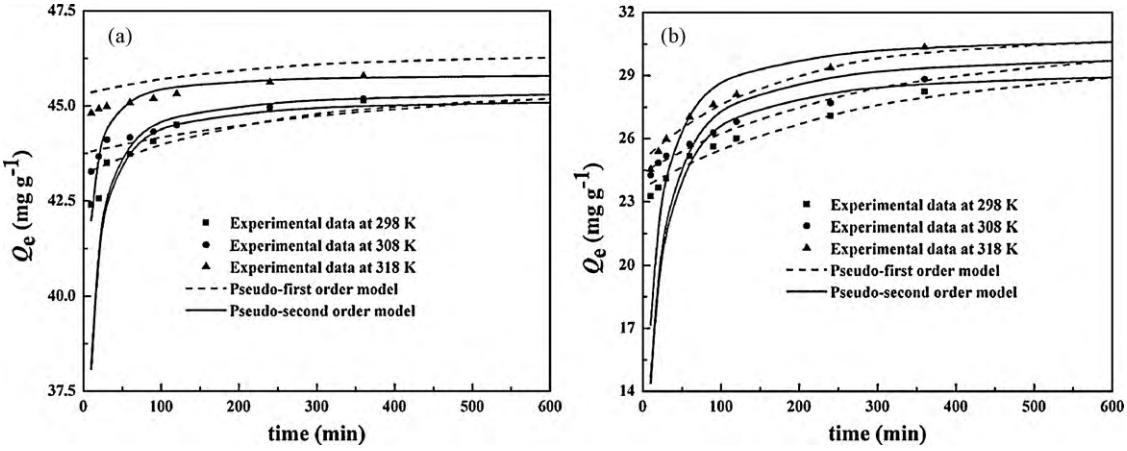

Fig. 5. Kinetic models of the effect of temperature on adsorption of 2,4-DCP onto MIP (a) and NIP (b).

Table 3
Kinetic parameters for the Pseudo-second-order equation.

Sorbents	Temperature (K)	u (mg g^{-1} min^{-1})	$t_{1/2}$ (h)	E_a (kJ mol^{-1})	r
MIP	298	23.91	1.901	27.63	0.8652
	308	24.52	1.864		
	318	50.57	0.9168		
NIP	298	2.875	10.38	8.116	0.7601
	308	2.908	10.55		
	318	3.801	8.132		

E_a could be evaluated by sloping of plot of $\ln k_2$ and versus $1/T$, which were found to be 27.63 kJ mol^{-1} for MIP and 8.116 kJ mol^{-1} for NIP. The initial adsorption rate and half-adsorption time are usually applied for a measure of adsorption rate. Furthermore, the value of *E*a for physics adsorption is often lower than that of chemical adsorption, and the initial adsorption rate for physics adsorption is affected slightly by temperature [31]. So the results indicated the adsorption process for MIP attributed to chemical adsorption, and the physics adsorption is the preferential process for NIP.

3.4.2. Intraparticle diffusion

The kinetic data can be used to study the presence or absence of intraparticle diffusion and to determine whether intraparticle diffusion is the rate-limiting step. A functional relationship common to most treatments intraparticle diffusion is described by Weber and Morris [32].

$$Q_t = k_i t^{0.5} + C \quad (16)$$

where k_i is the intraparticle diffusion rate constant (mg g^{-1} min$^{-0.5}$) and the intercept *C*, obtained by extrapolation of the linear portion of the plot of Q_t versus $t^{0.5}$, is an indicator to express the boundary layer thickness.

The intraparticle diffusion plots multi-linearity indicated that three steps were involved in the adsorption process for MIP (Fig. 6). The first, the initial stage can be attributed to the diffusion of 2,4-DCP through the solution to the external surface of MIP and diffusion of 2,4-DCP through the boundary layer to the surface of MIP [28]. The second stage described the gradual adsorption of 2,4-DCP and the intraparticle diffusion was the rate-limiting step. The last stage was attributed to the final equilibrium for which the intraparticle diffusion started to slow down due to extremely low concentration of 2,4-DCP left in solution. This kind of multi-linearity in the shape of the intraparticle diffusion plot was not observed in the adsorption of 2,4-DCP onto NIP (Fig. 6), indicating the effect of time for adsorption of 2,4-DCP onto MIP was more obviously than NIP.

3.5. Adsorption thermodynamics

Thermodynamic parameters such as change in Gibbs free energy (ΔG°), enthalpy (ΔH°) and entropy (ΔS°) were calculated using the following equations [23]:

$$\ln\left(\frac{Q_e}{C_e}\right) = \frac{\Delta S^\circ}{R} - \frac{\Delta H^\circ}{RT} \quad (17)$$

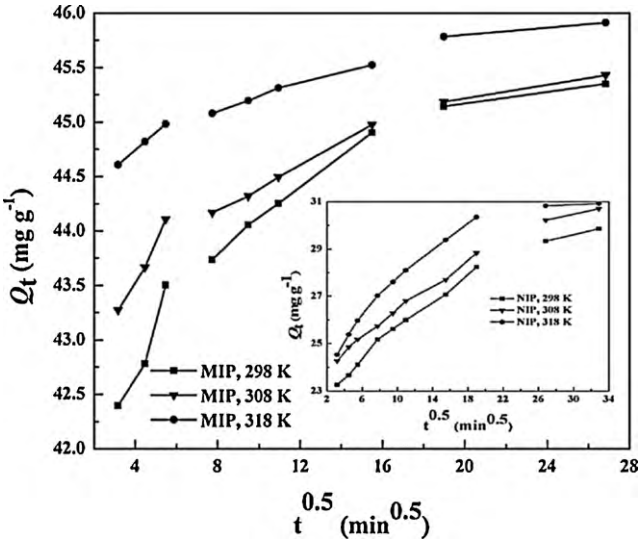

Fig. 6. Intraparticle diffusion treatment of 2,4-DCP onto MIP at various temperature. Inset: intraparticle diffusion treatment of 2,4-DCP onto NIP at various temperature.

$$\Delta G^\circ = \Delta H^\circ - T\Delta S^\circ \quad (18)$$

where *R* is the gas constant (8.314 J mol^{-1} K^{-1}) and *T* is the absolute temperature (K). Thus, ΔH° and ΔS° are obtained from the slope and intercept of the line plotted by $\ln(Q_e/C_e)$ versus $1/T$, respectively. The obtained thermodynamic parameters for MIP and NIP were listed in Table 4.

A negative ΔG° value indicated that the adsorption of 2,4-DCP was spontaneous within the temperature range evaluated, which was the case for many adsorption systems in solution. By adsorption abundant 2,4-DCP onto MIP surface, the number of water molecules surrounding 2,4-DCP molecules decreased and the degree of the freedom of the water molecules increased. Therefore, the positive values of ΔS° suggested increased randomness at the solid–solution interface during the adsorption 2,4-DCP onto MIP surface [33,34]. In fact, the positive value of enthalpy change ΔH° further confirmed the endothermic nature of the processes, so increasing temperature supplied with a more favourable adsorption between 2,4-DCP onto MIP.

Table 4
Thermodynamic parameters for the adsorption of 2,4-DCP onto MIP and NIP.

Sorbents	Temperature (K)	Thermodynamic parameters		
		ΔG (kJ mol^{-1})	ΔH (kJ mol^{-1})	ΔS (J mol^{-1} k^{-1})
MIP	298	−3.864	10.84	49.34
	308	−4.358		
	318	−4.851		
NIP	298	8.999	29.82	69.87
	308	8.301		
	318	7.602		

Table 5
Adsorption selectivity of MIP and NIP in a simulated effluent.

Phenolic compounds	MIP			NIP			k'
	C_e (mg L^{-1})	K_d (L g^{-1})	k	C_e (mg g^{-1})	K_d (mg L^{-1})	k	
24-DCP	10.46	4.279	–	56.99	0.3774	–	–
2,6-DCP	63.16	0.2916	14.67	76.20	0.1562	2.417	6.071
Phenol	87.16	0.0737	58.08	87.45	0.0717	5.261	11.04
4-CP	72.54	0.1892	22.61	78.49	0.1370	2.755	8.207

3.6. Selectivity studies of MIP towards 2,4-DCP

K_d, k and k' values were summarized in Table 5. From the data in Table 5, the following facts could be found: (i) The K_d and k values of MIP presented significant increase than those of NIP. This could be explained by the imprinting effect, abundant binding sites with functional groups in a predetermined orientation and special size were available for selective recognition of 2,4-DCP onto MIP. (ii) k' is an indicator to express the adsorption affinity of recognition sites to the template molecules. The k' results showed that the selective recognition of MIP for 2,4-DCP were nearly 6.071, 8.207 and 11.04 times greater than that of NIP. (iii) The k' values of MIP, for phenol and 4-CP in relation to 2,6-DCP, were greater. The results could be attributed to the fact that functional groups and molecular structure were similar between 2,6-DCP and 2,4-DCP. And the cavities imprinted by 2,4-DCP molecules on the surface of MIP were also suited to 2,6-DCP than phenol and 4-CP. The above results clearly revealed that MIP possessed high recognition and binding affinity for 2,4-DCP molecules.

3.7. Regeneration

The regeneration of sorbent, a key factor in improving value in use, was investigated in four sequential cycles of adsorption–desorption (Fig. SI). After four cycle's regeneration, the adsorption capacity of MIP for 2,4-DCP was about 8.111% loss in pure 2,4-DCP solution, about 10.73% loss in coexisting phenolic compounds solution. The MIP was shown to be promising for regeneration without significant loss in adsorption capacity, even in competitive environment.

4. Conclusions

In the present investigation, uniformly sized molecularly imprinted microspheres (MIP) were successfully prepared and evaluated as sorbent for recognitive adsorption of 2,4-DCP in aqueous solution. The results of characterization, kinetics, thermodynamics, selectivity and regeneration were summarized below:

(1) The molecularly imprinted microspheres, with uniformly sized diameter of 4.0 μm, were synthesized using β-cyclodextrin/attapulgite composites as support.
(2) The optimum condition for adsorption of 2,4-DCP was found to be pH 2.0. The proposed binding mechanism may be hydrogen bonding-electrostatic interactions, and the thermodynamic analysis presented the endothermic, spontaneous and entropy gained nature of the process.
(3) Equilibrium data were described by Langmuir, Freundlich and Dubinin–Radushkevich isotherm models, and the maximum adsorption capacity for MIP were 62.14 mg g^{-1}, 70.95 mg g^{-1} and 77.96 mg g^{-1} at 298 K, 308 K and 318 K, respectively.
(4) Kinetics experiments showed that MIP offered a fast kinetics for adsorption of 2,4-DCP, and a diffusion-controlled process as the essential adsorption rate-controlling step was also proposed.
(5) The selectivity studies suggested that the selective recognition of 2,4-DCP for MIP was nearly 6.0–11.0 times greater than that of NIP.
(6) MIP was applied in four cycle's regeneration without significant loss in adsorption capacity.

Acknowledgments

This work was financially supported by the National Natural Science Foundation of China (No. 20877036) and Ph.D. Programs Foundation of Ministry of Education of China (No. 20093227110015).

Appendix A. Supplementary data

Supplementary data associated with this article can be found, in the online version, at doi:10.1016/j.cej.2010.06.039.

References

[1] K. Abburi, Adsorption of phenol and p-chlorophenol from their single and bisolute aqueous solutions on Amberlite XAD-16 resin, J. Hazard. Mater. B 105 (2003) 143–156.
[2] Q.Z. Feng, L.X. Zhao, W. Yan, J.M. Lin, Z.X. Zheng, Molecularly imprinted solid-phase extraction combined with high performance liquid chromatography for analysis of phenolic compounds from environmental water samples, J. Hazard. Mater. (2009) 282–288.
[3] E. Caro, R.M. Marcé, F. Borrull, P.A.G. Cormack, D.C. Sherrington, Application of molecularly imprinted polymers to solid-phase extraction of compounds from environmental and biological samples, Trends Anal. Chem. 25 (2006) 143–154.
[4] Y. Li, X. Li, Y.Q. Li, J.Y. Qi, J. Bian, Y.X. Yuan, Selective removal of 2,4-dichlorophenol from contaminated water using non-covalent imprinted microspheres, Environ. Pollut. 157 (2009) 1879–1885.
[5] Q. Li, H.J. Su, T.W. Tan, Synthesis of ion-imprinted chitosan-TiO_2 adsorbent and its multi-functional performances, Biochem. Eng. J. 38 (2008) 212–218.
[6] K. Tsukagoshi, K.Y. Yu, M. Maeda, M. Takagi, Metal ion-selective adsorbent prepared by surface-imprinting polymerization, Bull. Chem. Soc. Jpn. 66 (1993) 114–120.
[7] Y.M. Ren, M.L. Zhang, D. Zhao, Synthesis and properties of magnetic Cu(II) ion imprinted composites adsorbent for selective removal of copper, Desalination 228 (2008) 135–149.
[8] G.H. Wu, Z.Q. Wang, J. Wang, C.Y. He, Hierarchically imprinted organic–inorganic hybrid sorbent for selective separation of mercury ion from aqueous solution, Anal. Chim. Acta 582 (2007) 304–310.
[9] X.J. Chang, N. Jiang, H. Zheng, Q. He, Z. Hu, Y.H. Zhai, Y.M. Cui, Solid-phase extraction of iron(III) with an ion-imprinted functionalized silica gel sorbent prepared by a surface imprinting technique, Talanta 71 (2007) 38–43.
[10] E. Birlik, A. Ersöz, E. Açıkkalp, A. Denizli, R. Say, Cr(III)-imprinted polymeric beads: sorption and preconcentration studies, J. Hazard. Mater. 140 (2007) 110–116.
[11] N. Candan, N. Tüzmen, M. Andac, C.A. Andac, R. Say, A. Denizli, Cadmium removal out of human plasma using ion-imprinted beads in a magnetic column, Mater. Sci. Eng. C 29 (2009) 144–152.
[12] Y.H. Zhai, Y.W. Liu, X.J. Chang, X.F. Ruan, J.L. Liu, Metal ion–small molecule complex imprinted polymer membranes: preparation and separation characteristics, React. Funct. Polym. 68 (2008) 284–291.
[13] J.H. Huang, Y.F. Liu, Q.Z. Jin, X.G. Wang, J. Yang, Adsorption studies of a water soluble dye, Reactive Red MF-3B, using sonication-surfactant-modified attapulgite clay, J. Hazard. Mater. 143 (2007) 541–548.
[14] H.M. Liu, C.H. Liu, X.J. Yang, S.J. Zeng, Y.Q. Xiong, W.J. Xu, Uniformly sized β-cyclodextrin molecularly imprinted microspheres prepared by a novel surface imprinting technique for ursolic acid, Anal. Chim. Acta 628 (2007) 87–94.
[15] B. Xu, W.M. Huang, Y.T. Pei, Z.G. Chen, A. Kraft, R. Reuben, J.Th.M. De Hosson, Y.Q. Fu, Mechanical properties of attapulgite clay reinforced polyurethane shape-memory nanocomposites, Eur. Polym. J. 45 (2009) 1904–1911.
[16] Y. Li, X. Li, C.K. Dong, Y.Q. Li, P.F. Jin, J.Y. Qi, Selective recognition and removal of chlorophenols from aqueous solution using molecularly imprinted polymer prepared by reversible addition-fragmentation chain transfer polymerization, Biosens. Bioelectron. 25 (2009) 306–312.
[17] W. Zhang, L. Qin, X.W. He, W.Y. Li, Y.K. Zhang, Novel surface modified molecularly imprinted polymer using acryloyl-β-cyclodextrin and acrylamide as monomers for selective recognition of lysozyme in aqueous solution, J. Chromatogr. A 1216 (2009) 4560–4567.
[18] M. Sathishkumar, A.R. Binupriya, D. Kavitha, R. Selvakumar, R. Jayabalan, J.G. Choi, S.E. Yun, Adsorption potential of maize cob carbon for 2,4-dichlorophenol removal from aqueous solutions: equilibrium, kinetics and thermodynamics modeling, Chem. Eng. J. 147 (2009) 265–271.
[19] C. Moreno-Castilla, Adsorption of organic molecules from aqueous solutions on carbon materials, Carbon 42 (2004) 83–94.
[20] M. Mazzotti, Equilibrium theory based design of simulated moving bed processes for a generalized Langmuir isotherm, J. Chromatogr. A 1126 (2006) 311–322.
[21] S.J. Allen, G. Mckay, J.F. Porter, Adsorption isotherm models for basic dye adsorption by peat in single and binary component systems, J. Colloid Interface. Sci. 280 (2004) 322–333.
[22] A.P. Terzyk, R. Wojsz, G. Rychlicki, P.A. Gauden, Fractal dimension of microporous carbon on the basis of Polanyi–Dubinin theory of adsorption. Dubinin–Radushkevich adsorption isotherm equation, Colloids Surf. A 119 (1996) 175–181.
[23] K.Q. Li, X.H. Wang, Adsorptive removal of Pb(II) by activated carbon prepared from *Spartina alterniflora*: equilibrium, kinetics and thermodynamics, Bioresour. Technol. 100 (2009) 2810–2815.
[24] Y.S. Ho, G. McKay, The sorption of lead(II) ions on peat, Water Res. 33 (1999) 578–584.
[25] Y.S. Ho, G. McKay, Pseudo-second order model for sorption processes, Process Biochem. 34 (1999) 451–465.

[26] A.E. Ofomaja, Sorption dynamics and isotherm studies of methylene blue uptake on to palm kernel fibre, Chem. Eng. J. 126 (2007) 35–43.
[27] A.E. Ofomaja, Kinetic study and sorption mechanism of methylene blue and methyl violet onto mansonia (*Mansonia altissima*) wood sawdust, Chem. Eng. J. 143 (2008) 85–95.
[28] A.E. Ofomaja, Intraparticle diffusion process for lead(II) biosorption onto mansonia wood sawdust, Bioresour. Technol. 101 (2010) 5868–5876.
[29] A.E. Ofomaja, Y.S. Ho, Effect of pH on cadmium biosorption by coconut copra meal, J. Hazard. Mater. 139 (2007) 356–362.
[30] Z.J. Wu, H. Joo, K. Lee, Kinetics and thermodynamics of the organic dye adsorption on the mesoporous hybrid xerogel, Chem. Eng. J. 112 (2005) 227–236.
[31] Y.H. Shu, X.H. Jia, The mechanisms for CTMAB-bentonites to adsorb CBs from water in the adsorption kinetics and thermodynamics view, Acta Sci. Circum. 25 (2005) 1530–1536.
[32] W.J. Weber Jr., J.C. Morris, Kinetics of adsorption on carbon from solution, J. Sanit. Eng. ASCE. 89 (1963) 31–42.
[33] A. Mellah, S. Chegrouche, M. Barkat, The removal of uranium(VI) from aqueous solutions onto activated carbon: kinetic and thermodynamic investigations, J. Colloid Interface Sci. 296 (2006) 434–441.
[34] J. Wu, H.Q. Yu, Biosorption of 2,4-dichlorophenol from aqueous solution by *Phanerochaete chrysosporium* biomass: isotherms, kinetics and thermodynamics, J. Hazard. Mater. B 137 (2006) 498–508.